

Electroosmotic Flows with Random Zeta Potential

James P. Gleeson

National Microelectronics Research Centre and Department of Applied Mathematics, University College Cork, Cork, Ireland

E-mail: j.gleeson@ucc.ie

Received September 12, 2001; accepted January 24, 2002; published online March 22, 2002

The hydrodynamic problem of electroosmotic flow in a cylindrical capillary with random zeta potential is solved in the limit of small Debye length and low Reynolds number. Averages are defined over multiple experiments and the mean axial velocity is found to be a plug flow. The variance of the velocity exhibits parabolic-like variation across the capillary. Average concentrations of samples transported by the flow are approximated by defining an effective diffusivity coefficient. Theoretical formulas for the average concentration are supported by numerical experiments.

© 2002 Elsevier Science (USA)

Key Words: electroosmosis; zeta potential; effective diffusivity.

1. INTRODUCTION

Capillary electroosmotic flow of an electrolyte arises when surface charges on the capillary wall attract a sheath of counterions in the fluid. The imposition of an electric field E parallel to the capillary wall then exerts a body force on the sheath and gives rise to a steady flow in the body of the fluid that is generally plug-like, i.e., exhibiting no variation with radial position r across the capillary. This plug flow profile is valid outside the Debye layer (or “electric double layer”) adjacent to the wall. Inside this layer the coupling of the fluid and electrostatic problems results in equations that do not generally admit analytic solutions. The analysis is considerably simplified for the case of very thin Debye layers—if the thickness of the layer is smaller than any other length scale, the problem may be reduced to a hydrodynamic flow problem with the electroosmotic sheath flow appearing only as a boundary condition relating the fluid velocity to the so-called zeta potential. In the frequently encountered case of low Reynolds number, the flow is described by the Stokes equations. These are linear equations and so analytical solutions may be found using transform methods.

Electroosmotic flows are extensively employed for fluid transport and sample separation in channels or capillaries with length scales on the order of 100 μm . Experimental flow imaging (1, 2) has determined the disruption of the plug flow profile as a result of inhomogeneities in the capillary wall surface. These effects generally consist of parabolic flow profiles replacing the plug flow, and result in the Taylor dispersion (3) of samples being

transported by the flow. Similar effects are seen in numerical simulations (4). Long *et al.* (5) considered the analytical solution of the Stokes equations for arbitrary surface inhomogeneity using Fourier transforms (6), and showed that localized surface defects introduce long-range perturbations to the flow. In this paper we consider a natural generalization of this work to capillaries with a random distribution of surface heterogeneities, modeled by a zeta potential that varies randomly (but with small variance) about its mean value along the capillary. The randomness of the zeta potential means that the velocity is essentially random also, and so is unpredictable in any single experiment. However, the distribution of measurements of the velocity over a large ensemble of experiments defines an average, with individual measurements scattered about the mean value. We show that the mean velocity has a plug-flow profile and that the variance of the velocity (i.e., the extent of experimental scatter) depends on the radial position in the capillary, as well as on the statistical characteristics of the zeta potential. If, in each experiment, an identical initial concentration of a passive (dye) tracer is added to the fluid, the velocity profile is clearly shown by the distortion of the dye as it moves down the capillary (1, 2). The extent of the distortion will vary from experiment to experiment, depending on the random velocity. Measurements across multiple experiments again define an ensemble average, and we show that the mean concentration profile can be approximated using methods from turbulent diffusion theory. The average concentration profile resembles that which would be found if the initial concentration profile was affected by a radial-dependent molecular diffusion. We stress that the average profile can only be found from a large ensemble of independent experiments, unlike the self-averaging in a single experiment of molecular diffusion, which causes the well-known Taylor dispersion of samples. In order to clarify the distinction between these two effects we take the molecular diffusion to be zero throughout most of this paper. The effects of relaxing this unphysical assumption are examined in Section 8.

The remainder of the paper is organized as follows. Section 2 briefly reviews the Stokes equations and Section 3 introduces the statistical quantities needed to characterize the flows. The solution of the Stokes equations (5, 6) is presented in Section 4, with the mean and variance of the fluid velocity calculated

in Section 5. The average scatter of samples is examined in Section 6 and supported by numerical simulations in Section 7. Section 8 briefly examines the effect of nonzero molecular diffusion upon the average scatter, followed by a summary and discussion of our results.

2. HYDRODYNAMIC EQUATIONS

Steady electroosmotic flow of an incompressible fluid in the limits of low Reynolds number and small Debye length may be described by the Stokes equations

$$\begin{aligned}\nabla p - \mu \nabla^2 \mathbf{v} &= 0, \\ \nabla \cdot \mathbf{v} &= 0,\end{aligned}\quad [1]$$

for pressure p , velocity vector \mathbf{v} , and viscosity μ , with suitable boundary conditions. We consider axisymmetric flow in a cylindrical capillary of radius a , with the axis oriented along the z direction, axial velocity $v(r, z)$, and radial velocity $u(r, z)$. The pressure at both ends of the capillary is the same, so there is no Poiseuille flow due to external pressure gradients. The effect of an electric field E applied along the capillary is then expressed as a slip boundary condition on the axial velocity at $r = a$

$$v(a, z) = -\frac{\epsilon}{\mu} E \zeta, \quad [2]$$

where ϵ is the dielectric constant of the electrolyte and ζ is the zeta potential of the surface. The zeta potential is commonly assumed to be constant along the length of the capillary, yielding the usual plug flow solution

$$\begin{aligned}v(r, z) &= -\frac{\epsilon}{\mu} E \zeta, \\ u(r, z) &= 0,\end{aligned}$$

which is independent of r and z . However, recent work (2, 4, 5) has highlighted the nonlocal effects on the flow of surface defects, i.e., variations in the value of ζ . We therefore take ζ to be a random function of z , with known mean $\bar{\zeta}$ and variance σ^2 , and derive in Section 5 the statistical characteristics of the velocity. The randomness of the velocity results in a statisti-

cal distribution of initially compact samples transported by the flow—we show in Section 6 that the distribution of the sample concentration over an ensemble of experiments may be predicted using methods from turbulence diffusion theory and related to the characteristics of the zeta potential.

3. RANDOM ZETA POTENTIAL

We begin by seeking solutions of Eq. [1] with the boundary condition at the capillary wall $r = a$ corresponding to slip flow with nonconstant zeta potential:

$$\begin{aligned}v(a, z) &= -\frac{\epsilon}{\mu} E \zeta(z), \\ u(a, z) &= 0.\end{aligned}\quad [3]$$

For convenience we nondimensionalize all lengths by writing them as multiples of the capillary radius a . Overbars will denote averages over multiple measurements (or “realizations”). Multiple measurements may be on different capillaries of similar manufacture, or at well-spaced intervals along a single capillary. We use ensemble averages throughout this paper, meaning that averages are calculating over all independent realizations.

We model the zeta potential in each experiment as a homogeneous random function of z that varies around its average value $\bar{\zeta}$. In order to quantify the variation away from the mean we use the variance σ^2 defined by

$$\overline{(\zeta - \bar{\zeta})^2} = \sigma^2. \quad [4]$$

Typically $\sigma/\bar{\zeta}$ will be small, so that at a crude level ζ can be approximated by $\bar{\zeta}$. In Fig. 1 we plot examples of random zeta functions against axial distance z , with $\bar{\zeta} = 1$ and $\sigma = 0.15$.

We require one further statistical characteristic to differentiate between the examples in Figs. 1a and 1b; this is the *correlation function* R defined by

$$\overline{[\zeta(z_1) - \bar{\zeta}][\zeta(z_2) - \bar{\zeta}]} = \sigma^2 R(z_1 - z_2), \quad [5]$$

where R is an even function with $R(0) = 1$. The correlation function typically decays to 0 as its argument increases, with a characteristic decay length l called the correlation length. For

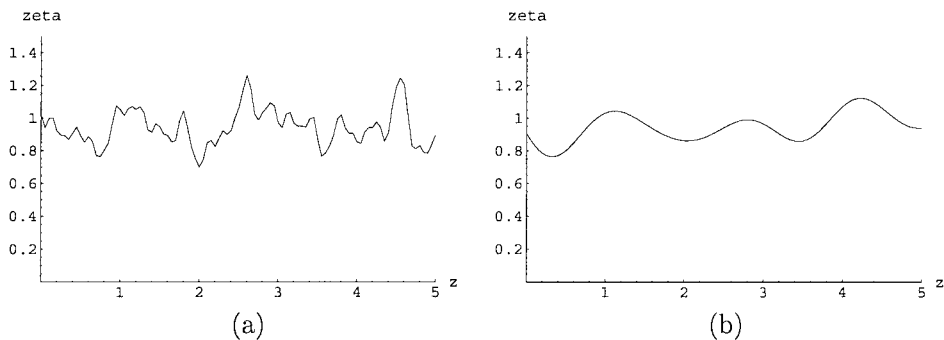


FIG. 1. Random zeta functions $\zeta(z)$, with mean $\bar{\zeta} = 1$, standard deviation $\sigma = 0.15$, and correlation lengths $l = 0.1$ (a) and $l = 0.5$ (b).

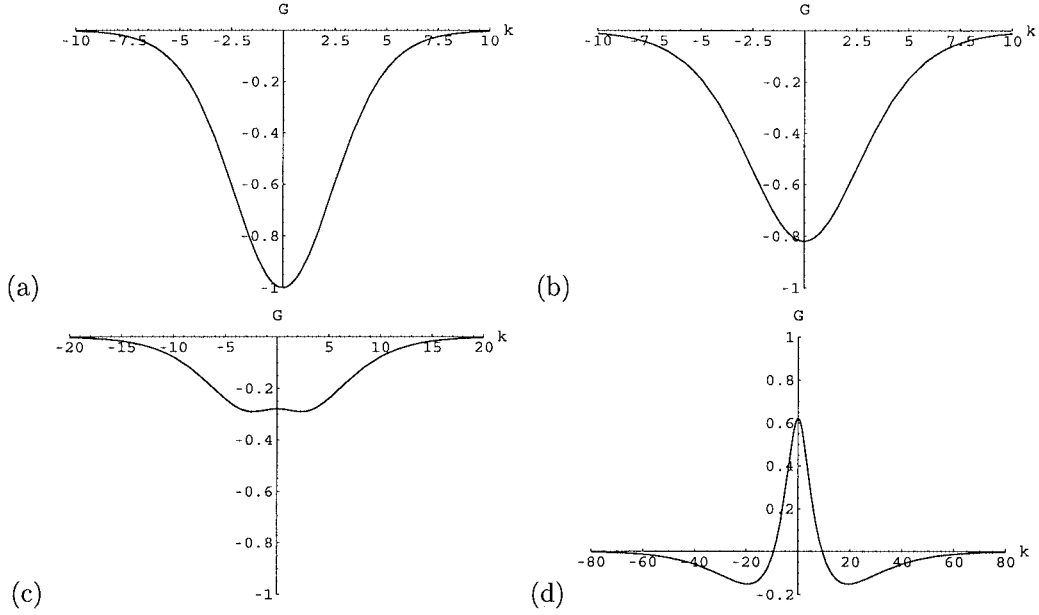


FIG. 2. The function $\hat{G}(r, k)$ for various values of r : (a) $r = 0$, (b) $r = 0.3$, (c) $r = 0.6$, and (d) $r = 0.9$.

definiteness (and to simplify the numerical experiments of Section 7), we choose the correlation function to have the form

$$R(z) = \exp\left(-\frac{z^2}{2l^2}\right). \quad [6]$$

Figure 1a then corresponds to the parameters $\bar{\zeta} = 1$, $\sigma = 0.15$, and $l = 0.1$, with Fig. 1b having $l = 0.5$. Note that the random effects remain correlated over longer distances in the second case—the length l may be thought of as a measure of how quickly the random function “forgets” its current value.¹

4. FLUID VELOCITY

The velocity at each point in the capillary may be derived from the zeta potential along the wall by employing the Fourier transform solutions of Eqs. [1], [3] as given in (5, 6). The transforms are defined by

$$\hat{v}(r, k) = \frac{1}{2\pi} \int_{-\infty}^{\infty} e^{-ikz} v(r, z) dz, \quad [7]$$

and the solutions for velocity components and pressure are then given in terms of the transform of the zeta potential:

$$\begin{aligned} \hat{v}(r, k) &= -\frac{\epsilon}{\mu} E \hat{G}(r, k) \hat{\zeta}(k), \\ \hat{u}(r, k) &= -\frac{\epsilon}{\mu} E \hat{F}(r, k) \hat{\zeta}(k), \\ \hat{p}(r, k) &= -\frac{\epsilon}{\mu} E \hat{H}(r, k) \hat{\zeta}(k). \end{aligned} \quad [8]$$

¹ The common (but physically unrealistic) limit of white noise is given by the limit $l \rightarrow 0$ with $\sigma \rightarrow \infty$, but keeping $\sigma^2 l$ constant.

The functions \hat{G} , \hat{F} , and \hat{H} are complicated combinations of Bessel functions of the first kind:

$$\begin{aligned} \hat{G}(r, k) &= \frac{I_0(kr)}{I_0(k)} + \frac{I_1(k)}{I_0(k)} \frac{k^2 r I_1(kr) I_0(k) - k^2 I_1(k) I_0(kr)}{k^2 I_1(k)^2 - k^2 I_0(k)^2 + 2k I_1(k) I_0(k)}, \\ \hat{F}(r, k) &= i \frac{I_1(k)}{k^2 I_1(k)^2 - k^2 I_0(k)^2 + 2k I_0(k) I_1(k)} \\ &\quad \times \left[k^2 \frac{I_0(k) I_1(kr)}{I_1(k)} - k^2 r I_0(k) \right], \\ \hat{H}(r, k) &= -2i \mu \frac{k^2 I_1(k) I_0(kr)}{k^2 I_1(k)^2 - k^2 I_0(k)^2 + 2k I_0(k) I_1(k)}. \end{aligned} \quad [9]$$

Figure 2 shows the form of \hat{G} as a function of k for different r values between the capillary axis $r = 0$ and the capillary wall $r = 1$. Note that $\hat{G}(r, k)$ decays to 0 for large k , and also that its value at $k = 0$ can be found from (9) to be

$$\hat{G}(r, 0) = 2r^2 - 1. \quad [10]$$

Finally, \hat{G} is an even function of k , i.e., $\hat{G}(r, -k) = \hat{G}(r, k)$.

Note that an implicit assumption in the use of transform methods is that the finite length of the capillary does not significantly affect the flow. This is generally true in experiments upon long, thin capillaries, provided that the measurements are not taken too close to the ends.

In theory the flow resulting from a given zeta potential may now be found by inverting [8]. However, the linearity of Eq. [1] means that any superposition of solutions is also a solution. In practice this means we must combine solutions so as to satisfy all the prescribed boundary conditions, and in particular to ensure that the pressure difference between ends of the capillary is zero.

We first invert [8] to yield an axial velocity and pressure given by

$$v(r, z) = -\frac{\epsilon}{\mu} E \int_{-\infty}^{\infty} e^{ikz} \hat{G}(r, k) \hat{\zeta}(k) dk,$$

$$p(r, z) = -\frac{\epsilon}{\mu} E \int_{-\infty}^{\infty} e^{ikz} \hat{H}(r, k) \hat{\zeta}(k) dk.$$

It can be shown (by considering the transform of the pressure gradient $ik\hat{p}$ at $k=0$) that this flow has a nonzero pressure difference between the ends of the capillary; in order to restore the pressure difference to 0 we therefore add a Poiseuille flow to get our final solution

$$v(r, z) = -\frac{\epsilon}{\mu} E \int_{-\infty}^{\infty} e^{ikz} \hat{G}(r, k) \hat{\zeta}(k) dk + 2\frac{\epsilon}{\mu} E (r^2 - 1) \hat{\zeta}(0). \quad [11]$$

This is the axial velocity solving [1], with slip boundary condition [3], and zero pressure difference between the ends of the capillary. The radial velocity u may be found similarly. Note the DC Fourier component $\hat{\zeta}(0)$ is the value of the zeta potential averaged over the length of the capillary in question—we assume this value is the same in each experiment (i.e., capillaries are of similar manufacture), and so $\hat{\zeta}(0) = \bar{\zeta}$.

5. RANDOM VELOCITY

Given a single realization of a random zeta potential $\zeta(z)$ (for example, as in Fig. 1) the velocity components u and v can be found using [11] and [8]. In Fig. 3 the nondimensionalization $\epsilon E \bar{\zeta} / \mu = -1$ is employed, and the vector field with horizontal (axial) component $v - 1$ and vertical (radial) component u corresponding to a single realization of a random zeta potential is plotted. The magnitude of the vectors is on the order of σ (with $\sigma = 0.15$ here), and so this is a small but significant secondary flow imposed upon the primary plug flow $v = 1$, $u = 0$ that

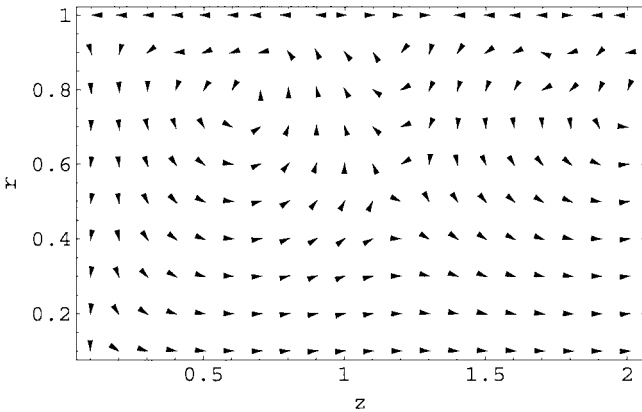


FIG. 3. Typical secondary flow induced by a random zeta potential at the wall, with parameters $\bar{\zeta} = 1$, $\sigma = 0.15$, and $l = 0.1$.

would occur if the zeta potential was constant. Recirculating flows may occur, but note the incompressibility of the velocity ensures the mass flux through any cross section of the capillary is constant.

Equation [11] formally gives us the axial velocity corresponding to a given random zeta potential $\zeta(z)$. As our information on the zeta potential is purely statistical in nature, the predictions of the velocity must also be of this form, i.e., yielding the average velocity and its variance and correlation function. We stress again that the averaging procedure used here is over an ensemble of experiments, i.e., a large number of experiments on capillaries of similar manufacture, or possible at a large number of well-separated sites on a single capillary.

We begin by Fourier transforming the statistical characteristics of the zeta potential for use in later calculations. The mean value of the zeta potential is the constant $\bar{\zeta}$, so the Fourier transform is

$$\overline{\hat{\zeta}(k)} = \delta(k) \bar{\zeta}, \quad [12]$$

with the Dirac delta function defined by

$$\delta(k) = \frac{1}{2\pi} \int_{-\infty}^{\infty} e^{-ikz} dz.$$

The correlation function R is defined by Eq. [5], which Fourier transforms to

$$\overline{\hat{\zeta}(k) \hat{\zeta}(k')} - \delta(k) \delta(k') \bar{\zeta}^2 = \delta(k + k') \sigma^2 \hat{R}(k), \quad [13]$$

with our model for the correlation function [6] transforming to

$$\hat{R}(k) = \frac{l}{\sqrt{2\pi}} \exp\left(-\frac{1}{2} k^2 l^2\right). \quad [14]$$

These results are now used to find the mean and variance of the axial velocity v . First, averaging [11] and using [10] gives the mean velocity.

$$\begin{aligned} \overline{v(r, z)} &= -\frac{\epsilon}{\mu} E \int_{-\infty}^{\infty} e^{ikz} \hat{G}(r, k) \delta(k) \overline{\hat{\zeta}(k)} dk + 2\frac{\epsilon}{\mu} E (r^2 - 1) \bar{\zeta} \\ &= -\frac{\epsilon}{\mu} E \bar{\zeta} [\hat{G}(r, 0) - 2(r^2 - 1)] \\ &= -\frac{\epsilon}{\mu} E \bar{\zeta}. \end{aligned} \quad [15]$$

This implies that the mean axial velocity is a plug flow. The measured values of the velocity are scattered randomly about this average, and so we calculate the variance of the velocity as an estimate of the extent of the experimental scatter. In fact we will find the velocity correlation function at two points z_1 and

z_2 , and then can easily find the variance by letting $z_1 = z_2$. From [11] we have

$$\begin{aligned} & [v(r, z_1) - \bar{v}][v(r, z_2) - \bar{v}] \\ &= \left(\frac{\epsilon}{\mu}E\right)^2 \left[\int_{-\infty}^{\infty} \int_{-\infty}^{\infty} e^{ik(z_1+z_2)} \hat{G}(k) \hat{G}(k') \hat{\xi}(k) \hat{\xi}(k') dk dk' \right. \\ & \quad - (2r^2 - 1) \bar{\xi} \int_{-\infty}^{\infty} e^{ikz_1} \hat{G}(k) \hat{\xi}(k) dk - (2r^2 - 1) \bar{\xi} \\ & \quad \left. \times \int_{-\infty}^{\infty} e^{ik'z_2} \hat{G}(k') \hat{\xi}(k') dk' + (2r^2 - 1)^2 \bar{\xi}^2 \right]. \quad [16] \end{aligned}$$

Taking the average of this, using [13], [12], and [10] yields

$$\begin{aligned} & \overline{[v(r, z_1) - \bar{v}][v(r, z_2) - \bar{v}]} \\ &= \left(\frac{\epsilon}{\mu}E\right)^2 \sigma^2 \int_{-\infty}^{\infty} e^{ik(z_1-z_2)} \hat{G}(r, k)^2 \hat{R}(k) dk \\ &= \frac{\bar{v}^2 \sigma^2}{\bar{\xi}^2} \int_{-\infty}^{\infty} e^{ik(z_1-z_2)} \hat{G}(r, k)^2 \hat{R}(k) dk, \quad [17] \end{aligned}$$

and so the velocity variance is

$$\begin{aligned} \overline{[v(r, z) - \bar{v}]^2} &= \frac{\bar{v}^2 \sigma^2}{\bar{\xi}^2} \int_{-\infty}^{\infty} \hat{G}(r, k)^2 \hat{R}(k) dk \\ &= \frac{\bar{v}^2 \sigma^2}{\bar{\xi}^2} f(r). \quad [18] \end{aligned}$$

Note that the integral depends on r ; i.e., the amount of variation of v about its mean depends on the radial measurement position. Figure 4 shows the dimensionless function

$$f(r) = \int_{-\infty}^{\infty} \hat{G}(r, k)^2 \hat{R}(k) dk \quad [19]$$

calculated by the numerical integration at each value of r . The variations are generally largest in the middle and at the sides of

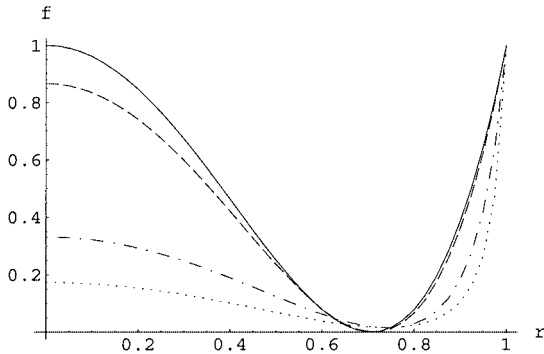


FIG. 4. The function $f(r)$ for various values of the correlation length l : $l = 10$ (solidline), $l = 1$ (dashedline), $l = 0.2$ (dot-dashline), and $l = 0.1$ (dottedline). The comparison function $(1 - 2r^2)^2$ is indistinguishable from the solid line.

TABLE 1
Values of $f(r)$ for Various r and l

	$r = 0$	$r = 0.25$	$r = 0.5$
$l = 0.1$	0.173	0.143	0.069
$l = 0.2$	0.331	0.271	0.124
$l = 0.3$	0.465	0.377	0.162
$l = 0.4$	0.573	0.460	0.187
$l = 0.5$	0.657	0.524	0.204
$l = 1$	0.866	0.674	0.236
$l = 5$	0.993	0.761	0.249
$l = 10$	0.998	0.765	0.250

the capillary, with a minimum near $r = 1/\sqrt{2}$. Also plotted for comparison is the parabolic-squared function $(1 - 2r^2)^2$, which is approached by $f(r)$ in the limit $l \rightarrow \infty$. It is clear that the value of $f(r)$, and so of the velocity variance, depends strongly on the statistical characteristics σ^2 and l of the zeta potential, and we propose that measurements of velocity variance at various radial positions could be used to estimate σ^2 and l . With this application in mind, a table of values of $f(r)$ for various r and l is provided in Table 1. Experiments to find the velocity variance would involve measurements of the velocity over multiple capillaries, and at various radial positions. Averages calculated over the whole ensemble of experiments should yield a mean velocity that is independent of radial position (average plug flow). However, the experimental results are scattered about the mean value, and it is the variance of this scatter that gives the function $f(r)$ defined in [18]. In the following sections we model one possible method of measuring the velocity, viz. following a passive dye tracer as it flows through the capillary. We show that the mean dye concentration is related to the velocity variance, and so to the statistics of the zeta potential through Eq. [18].

6. AVERAGE CONCENTRATION OF TRACERS

We have established that the variance of the axial velocity v depends on r . The effect of this variance is measurable when passive tracers are added to the steady fluid flow, e.g., dye tracers, such as those used in recent flow visualization experiments (1, 2). Consider an initial distribution of tracers $\theta_0(r, z)$ at time $t = 0$. These tracers will attempt to follow the fluid streamlines, but diffuse away from them because of molecular diffusion (Brownian motion). The equation specifying the concentration $\theta(r, z, t)$ in each experiment is

$$\frac{\partial \theta}{\partial t} + \mathbf{v} \cdot \nabla \theta - \kappa_0 \nabla^2 \theta = 0, \quad [20]$$

where κ_0 is the molecular diffusivity and the velocity is given by [8]. For clarity we will set $\kappa_0 = 0$ in most of the following (but see Section 8), thus ensuring the tracers follow the flow exactly. We imagine now a whole ensemble of experiments, each using a different capillary, but all with the same initial concentration profile θ_0 . The concentration profile will be distorted in

a different way in each experiment, but we are interested in the mean profile $\bar{\theta}$ found by averaging the measured concentration over the ensemble of experiments. We also restrict our attention to initial concentrations $\theta_0(z)$ that are uniform across the capillary—this is commonly the case in experiments and means that the effects of randomness in the radial direction are much smaller than in the axial direction.

In each experiment the tracers move along the random streamlines of the fluid, distorting the concentration profile away from its original form and introducing transverse variations. Although in each individual experiment the distortion is random, the average profile over the ensemble is predictable, and may therefore be experimentally tested. Methods in the theory of turbulent diffusion to approximate the average profile $\bar{\theta}$ found in an ensemble of experiments have been developed (7, 8). One approach is to define an *effective diffusivity coefficient* $D(r, t)$ so that $\bar{\theta}$ is approximated by the solution of the diffusion equation

$$\frac{\partial \bar{\theta}}{\partial t} + \bar{v} \frac{\partial \bar{\theta}}{\partial z} - \frac{D}{2} \frac{\partial^2 \bar{\theta}}{\partial z^2} = 0. \quad [21]$$

This equation has the solution

$$\bar{\theta} = \frac{1}{\sqrt{2\pi D(r, t)}} \int_{-\infty}^{\infty} \theta_0(z') \exp\left[-\frac{(z - \bar{v}t - z')^2}{2D(r, t)}\right] dz', \quad [22]$$

and so the effective diffusivity allows us to predict the mean profile $\bar{\theta}$, given only the initial profile θ_0 . Note that Eq. [21] applies only to the *average* of the experiments; in each individual experiment the concentration is found using Eq. [20]. Moreover, the effective diffusivity in the radial direction has been neglected, because the initial concentrations $\theta_0(z)$ is independent of r , and for $\sigma \ll \bar{\zeta}$ recirculating flows occur only rarely. Therefore the radial positions of tracers change relatively little compared to their axial motion and the average concentration profile exhibits significant change only in the axial direction:

$$\frac{\partial \bar{\theta}}{\partial r} \ll \frac{\partial \bar{\theta}}{\partial z}. \quad [23]$$

Thus we are justified in making the simplifying assumption that the radial effective diffusivity may be neglected in [21], but note that radial dependence is retained through the dependence of D itself upon r .

The problem now is to find an expression for the effective diffusivity D . Approximate expressions for effective diffusivities may be developed using a number of approaches, in particular (8) defined a series expansion for D of the form

$$D = D_1 + D_2 + \dots, \quad [24]$$

with each D_i defined by repeated integration of the Fourier transforms of the velocity variance [17]. The result for D_1 is

$$D_1(r, t) = 2 \frac{\bar{v}^2 \sigma^2}{\bar{\zeta}^2} \int_{-\infty}^{\infty} \hat{G}(r, k)^2 \hat{R}(k) \frac{1 - \cos(\bar{v}kt)}{\bar{v}^2 k^2} dk, \quad [25]$$

and for the cases examined here D_1 dominates the series expansion, so that $D \simeq D_1$ (provided that the random effects are relatively small, $\sigma \ll \bar{\zeta}$). Figure 5a shows the diffusivity D_1 (multiplied by $\bar{\zeta}^2/\sigma^2$) as a function of nondimensional time $\bar{v}t$ for various r positions across the capillary. Note that the diffusivity soon reaches a constant slope, the value of which depends on r . This dependence can be shown in [25] by changing the variable of integration from k to $q = \bar{v}kt$, so that the diffusivity is

$$D_1(r, t) = 2\bar{v}t \frac{\sigma^2}{\bar{\zeta}^2} \int_{-\infty}^{\infty} \hat{G}\left(r, \frac{q}{\bar{v}t}\right)^2 \hat{R}\left(\frac{q}{\bar{v}t}\right) \frac{1 - \cos(q)}{q^2} dq. \quad [26]$$

In the limit $t \rightarrow \infty$ this becomes

$$\begin{aligned} D_1(r, t) &\sim 2\bar{v}t \frac{\sigma^2}{\bar{\zeta}^2} \hat{G}(r, 0)^2 \hat{R}(0) \int_{-\infty}^{\infty} \frac{1 - \cos(q)}{q^2} dq \\ &= 2\bar{v}t \frac{\sigma^2}{\bar{\zeta}^2} (2r^2 - 1)^2 l \sqrt{\frac{\pi}{2}}. \end{aligned} \quad [27]$$

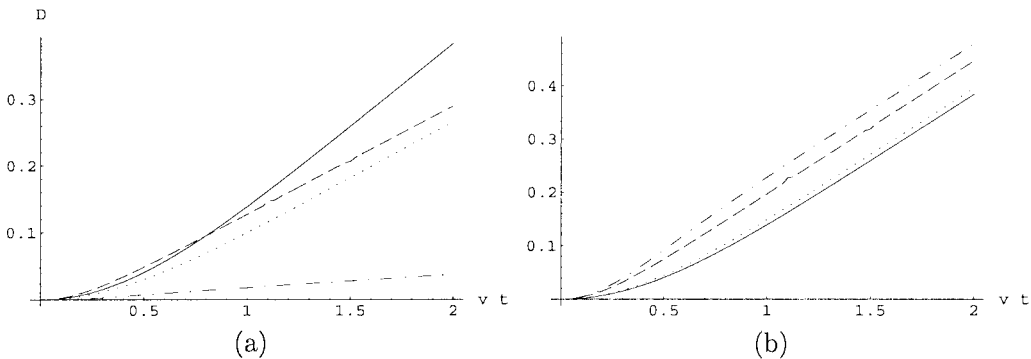


FIG. 5. (a) Normalized diffusivity $\bar{\zeta}^2 D/\sigma^2$ for $l = 0.1$ at $r = 0$ (solidline), $r = 0.3$ (dottedline), $r = 0.6$ (dot-dashline), and $r = 0.95$ (dashedline). (b) Same as (a), but for the function $\bar{\zeta}^2 D/(\sigma^2(2r^2 - 1)^2)$.

To confirm this r dependence we plot in Fig. 5b the function

$$\frac{\bar{\zeta}^2}{\sigma^2} \frac{D_1}{(2r^2 - 1)^2},$$

which clearly approaches a constant (and r -independent) slope at large times. For small times, the integrand in [25] may be expanded as a Taylor series in $\bar{v}t$, yielding

$$\begin{aligned} D_1(r, t) &\simeq 2 \frac{\bar{v}^2 \sigma^2}{\bar{\zeta}^2} \int_{-\infty}^{\infty} \hat{G}(r, k)^2 \hat{R}(k) \frac{1}{2} t^2 dk \\ &= \frac{\bar{v}^2 \sigma^2}{\bar{\zeta}^2} f(r) t^2 \text{ as } t \rightarrow 0. \end{aligned} \quad [28]$$

To demonstrate the effect of the effective diffusivity approximation [21] we consider an initial concentration given by

$$\theta_0(z) = \begin{cases} 1 & 0 < z < 0.2 \\ 0 & \text{otherwise,} \end{cases} \quad [29]$$

in a flow with mean velocity $\bar{v} = 1$, and random zeta potential with parameters $\bar{\zeta} = 1$, $\sigma = 0.15$, and $l = 0.1$. This initial profile is distorted in an unpredictable manner in each realization, but the mean profile found by averaging over all experiments is given by Eq. [22],

$$\begin{aligned} \bar{\theta}(r, z, t) &= \frac{1}{\sqrt{2\pi D(r, t)}} \int_0^{0.2} \exp\left[-\frac{(z-t-z')^2}{2D(r, t)}\right] dz' \\ &= \frac{1}{2} \operatorname{erf}\left(\frac{z-t}{\sqrt{2D(r, t)}}\right) - \frac{1}{2} \operatorname{erf}\left(\frac{z-0.2-t}{\sqrt{2D(r, t)}}\right). \end{aligned} \quad [30]$$

This average concentration profile is plotted at times $t = 0.4$ and $t = 2$ in Fig. 6.

In many experiments it is not possible to measure the concentration at individual r points in the interior of the capillary; instead a cross-section average is generally calculated. We therefore define the *average cross-section concentration* as

$$\langle \bar{\theta} \rangle = 2 \int_0^1 r \bar{\theta}(r, z, t) dr, \quad [31]$$

where the angle brackets refer to the cross-section averaging procedure. This $\langle \bar{\theta} \rangle$ is a function of z and t and can be found by plugging [30] into [31] and integrating. The resulting average cross-section concentration is plotted in Fig. 7. In the next section we compare these theoretical results with numerical simulations of actual flows and find good agreement.

7. NUMERICAL SIMULATIONS

As a check on the theoretical results presented in Section 6 and to show the concentration profile in typical individual experiments, we solve Eq. [20] with $\kappa_0 = 0$ and initial condition [29] using a standard numerical method, over a large number N_r of realizations. In each realization a random zeta potential is generated by a sum over N_m random Fourier modes:

$$\zeta(z) = \bar{\zeta} + \frac{1}{\sqrt{N_m}} \sum_{n=1}^{N_m} A_n \cos(k_n z) + B_n \sin(k_n z),$$

where k_n , A_n , and B_n are taken from independent Gaussian

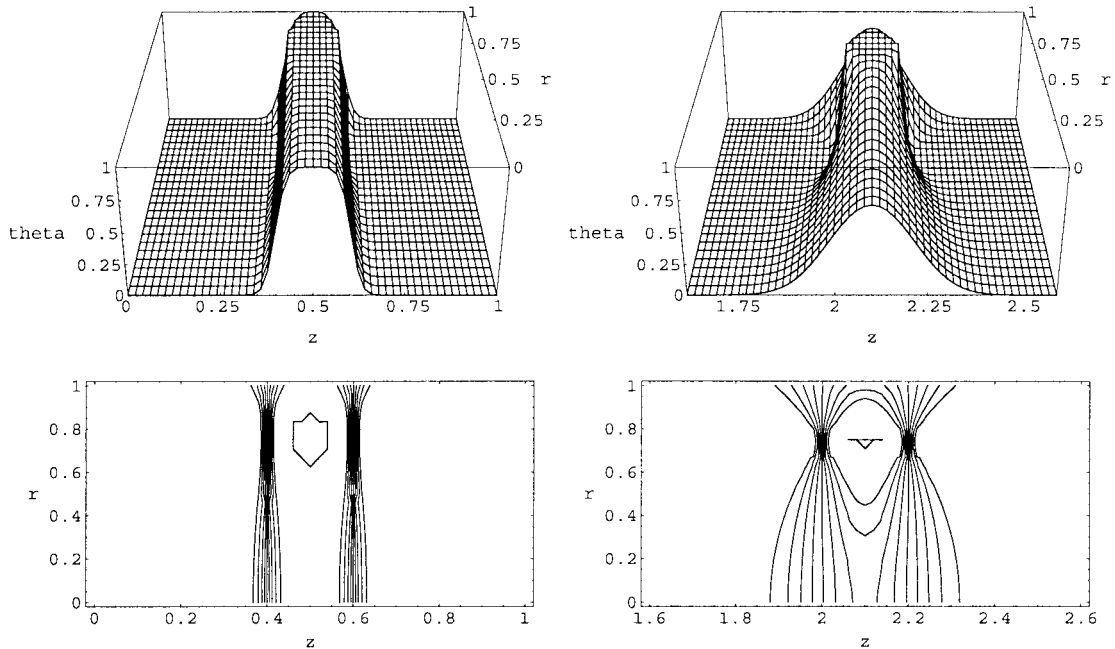


FIG. 6. Averaged concentration $\bar{\theta}$ and corresponding contours at $t = 0.4$ (left) and $t = 2.0$ (right).

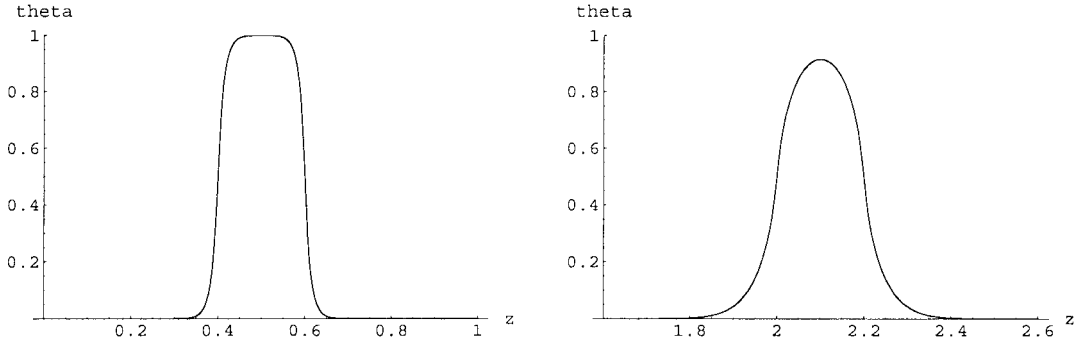


FIG. 7. Average cross-section concentrations ($\bar{\theta}$) at $t = 0.4$ (left) and $t = 2.0$ (right).

distributions with variances l^{-2} , σ^2 , and σ^2 , respectively. Lengths and times are nondimensionalized so that the capillary radius is one, and the average velocity \bar{v} is unity. It was found that $N_m = 50$ modes was sufficient to give a realistic random function, see Fig. 1 for examples. The velocity is then constructed by inverting [8] and a predictor–corrector method (8) is used to evolve the concentration $\theta(r, z, t)$ forward in time according to [20]. Each realization is the analogue of an experiment on a single capillary—an initial dye profile of form [29] is released in each capillary, and its profile is recorded at later times, see Fig. 8. Note the parabolic-like profile. The average concentration profile $\bar{\theta}$ is computed using 100 realizations (Fig. 9 and 10)—the results closely resemble the theoretical predictions of Eq. [31], compare to Figs. 6 and 7. In particular, note the mean profile has a similar shape to $f(r)$ at $t = 0.4$ as predicted by [28], but at $t = 2.0$ the long-time form due to [27] has emerged. These results imply that the average effect of the velocity variance [18] is detectable in the average tracer profile, and that the effects of the random zeta potential upon it are quite accurately modeled by the diffusion equation [21].

8. EFFECTS OF MOLECULAR DIFFUSION

All our work thus far has assumed that the molecular diffusivity κ_0 of the tracer is zero. As this will never be precisely the case in experimental situations, we consider briefly in this section the effects of nonzero κ_0 on our results.

Nonzero κ_0 causes dispersion of compact samples in every experiment, in contrast to the effects of the random zeta potential, which are visible (and give dispersive-like results) only when considering averages over the whole ensemble of experiments. We must therefore consider whether the effects of randomness in the zeta potential might be overshadowed by the diffusion due to κ_0 .

The series expansion [24] for D can be generalized for the case of nonzero κ_0 (8), the first terms are then

$$D(r, t) \simeq 2\kappa_0 t + 2 \frac{\bar{v}^2 \sigma^2}{\bar{\zeta}^2} \int_{-\infty}^{\infty} \hat{G}(r, k)^2 \hat{R}(k) \times \int_0^t (t - t') \exp(-\kappa_0 k^2 t') \cos(\bar{v} k t') dt' dk, \quad [32]$$

which reduces to [25] in the limit $\kappa_0 \rightarrow 0$. This formula can be used to generate plots of the diffusivity similar to Fig. 5. As an example, we plot in Fig. 11 the normalized diffusivity $\bar{\zeta}^2 D/\sigma^2$ at $r = 0$ for $l = 0.1$, with molecular diffusivity $\kappa_0 = 0.001$. This means that the Péclet number (returning to dimensional lengths) is

$$\frac{\bar{v}a}{\kappa_0} = 1000,$$

which we have chosen to correspond closely to the parameters of the example in Fig. 2 of Potoček *et al.* (4). Their capillary radius is $75 \mu\text{m}$, with (molecular) diffusion coefficient

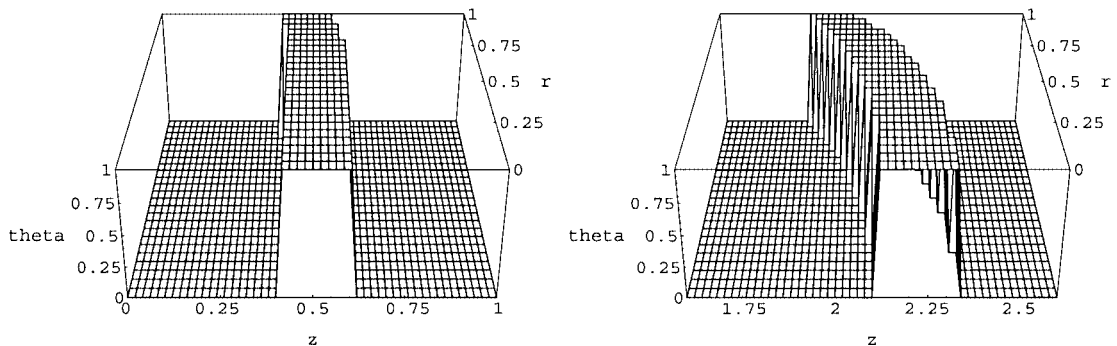


FIG. 8. A typical realization of the concentration θ at times $t = 0.4$ (left) and $t = 2.0$ (right).

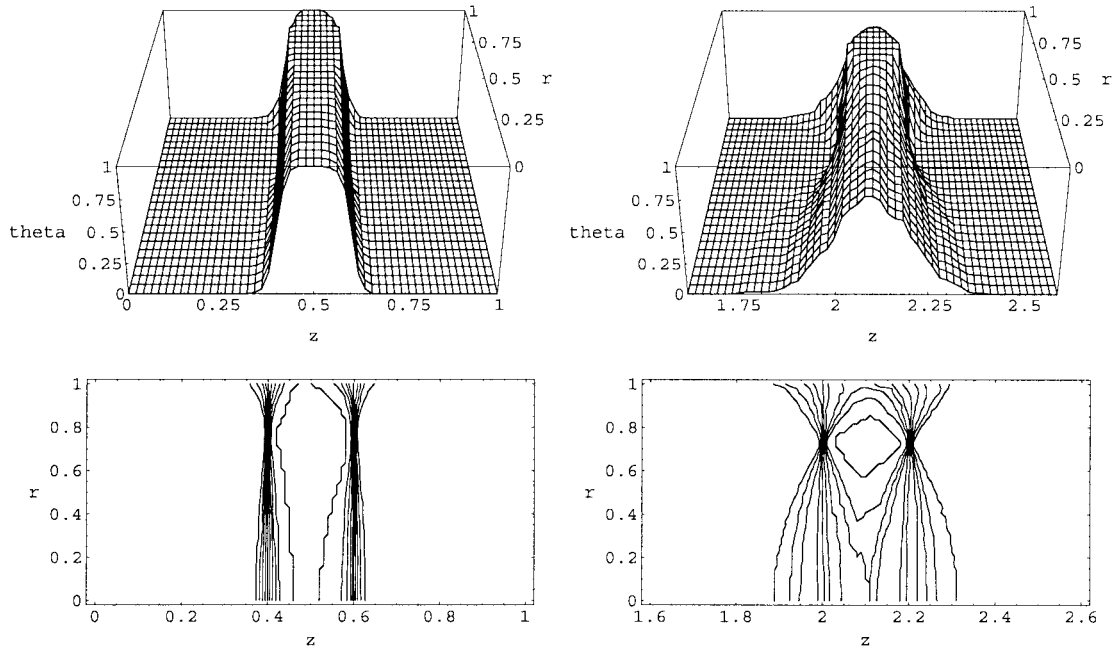


FIG. 9. Average (over 100 realizations) of the concentration $\bar{\theta}$ and corresponding contours at $t = 0.4$ (left) and $t = 2.0$ (right).

$\kappa_0 = 5 \times 10^{-11} \text{ m}^2 \text{ s}^{-1}$ and mean sample velocity on the order of $\bar{v} = 0.7 \text{ mm s}^{-1}$. We also plot for comparison the dispersion due solely to molecular diffusion, i.e., ignoring effects induced by the random zeta potential. We see that the effective diffusivity due to the random zeta potential is on the same order as the molecular diffusion, and so we would expect the effects of the randomness to remain detectable even in the presence of molecular diffusion, provided the Péclet number is sufficiently large.

9. DISCUSSION

We have demonstrated that the average electroosmotic flows in the presence of axially varying zeta potentials are plug-like, but with velocity variances that depend on radial position across the capillary. Averages are over an ensemble of capillaries of

similar manufacture (so all have the same mean zeta potential $\bar{\zeta}$). Equation [18] and Table 1 relate the velocity variance to the statistical characteristics of the zeta potential, and raise the possibility of inverting these relationships to gain information on the zeta potential from accurate measurements of the electroosmotic velocity.

One measurement technique involves the use of tracers in the fluid (1, 2). The variance in the velocity means that the tracer concentration profiles at a given time vary from individual experiment to individual experiment. We have shown that this random scatter in the concentration profile is related to the statistical characteristics of the zeta potential, see Eq. [25], and propose that measurements of the scatter could be used to estimate l , R , and σ by comparing with the average concentration found by solving Eq. [21]. All these results were achieved in the limit of zero molecular diffusivity (infinite Péclet number), but we

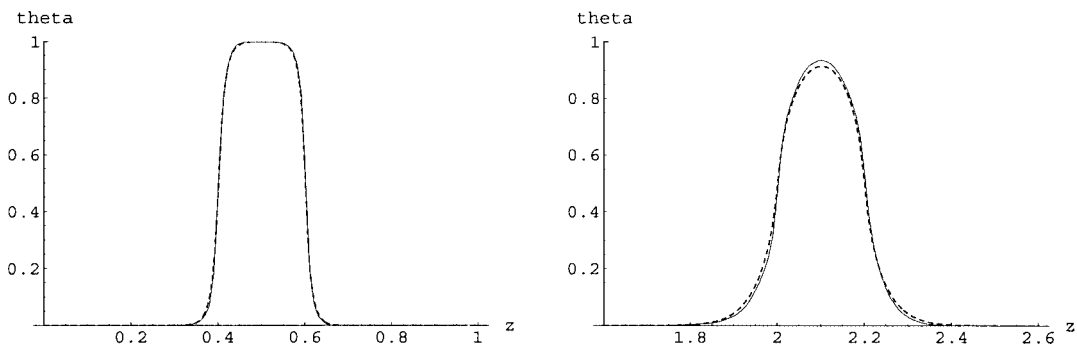


FIG. 10. Average cross-section concentration ($\bar{\theta}$) at $t = 0.4$ (left) and $t = 2.0$ (right). Numerical results (solidline) are close to the theoretical predictions (dottedline) from Fig. 7.

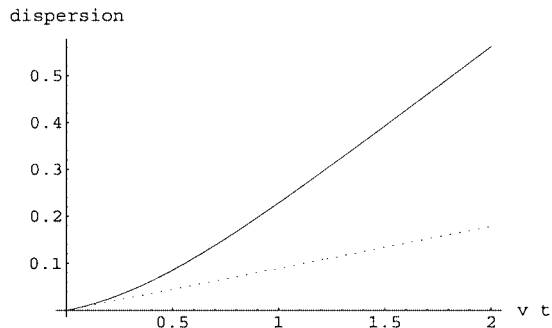


FIG. 11. Normalized diffusivity $\bar{\zeta}^2 D/\sigma^2$ with molecular diffusivity $\kappa_0 = 0.001$ (solidline) and the dispersion due solely to molecular diffusion (dotted-line). Here $\sigma = 0.15$, $r = 0$, and $l = 0.1$.

have shown that the effects of the random zeta potential remain detectable in the presence of a small molecular diffusivity κ_0 .

The assumptions made in this paper and necessary conditions for their validity are as follows:

1. We assume small Reynolds number and short Debye length. In particular, the Debye length must be smaller than any other characteristic length for the Stokes flow approximation to be valid. Typical Debye lengths are on the order of a nanometer (6), so our work should apply to zeta potentials with correlation lengths on the order of $0.1 \mu\text{m}$ and larger. Note that the dimensionless value $l = 0.1$ considered in the numerical examples would represent a correlation length of $10 \mu\text{m}$ in a typical $100\text{-}\mu\text{m}$ diameter capillary.

2. Secondary flow induced by the random zeta potential is much smaller than the primary plug flow. This means that recirculating flows occur with very small probability and so do not significantly affect the average over the ensemble. This allows the effective diffusivity in the radial direction to be neglected, and requires variations in ζ to be small, i.e.,

$$\sigma \ll \bar{\zeta}. \quad [33]$$

3. The series expansion [24] for the effective diffusivity D is well approximated by its first term if $D1 \gg D_2$. This requires

that

$$\frac{\sigma^2 l}{\bar{\zeta}^2 a} \ll 1. \quad [34]$$

4. As discussed briefly in Section 8, the dispersion due to the random zeta potential must be at least on the same order of magnitude as the molecular diffusion in order for the effects described in Section 6 to be experimentally measurable. This implies that

$$\frac{\sigma^2 \bar{v} l}{\bar{\zeta}^2 \kappa_0} \geq 1. \quad [35]$$

Note that this may be satisfied simultaneously with [34] provided that the Péclet number is very large:

$$Pe = \frac{\bar{v} a}{\kappa_0} \gg 1. \quad [36]$$

ACKNOWLEDGMENTS

The comments of an anonymous referee have greatly influenced the final version of this paper. This work was partially supported by the Faculty of Arts Research Fund and the Institute of Nonlinear Science, University College Cork and by the Irish HEA Programme for Research in Third Level Institutions Cycle 1: University College Cork Nanoscale Science and Technology Initiative.

REFERENCES

1. Paul, P. H., Garguilo, M. G., and Rakestraw, D. J., *Anal. Chem.* **70**, 2459 (1998).
2. Herr, A. E., Mohlo, J. I., Santiago, J. G., Mungal, M. G., and Kenny, T. W., *Anal. Chem.* **72**, 1053 (2000).
3. Taylor, G. I., *Proc. R. Soc. A* **219**, 186 (1953).
4. Potoček, B., Gaš, B., Kennler, E., and Štěrý, M., *J. Chromatogr. A* **709**, 51 (1995).
5. Long, D., Stone, H. A., and Ajdari, A., *J. Colloid Interface Sci.* **212**, 338 (1999).
6. Anderson, J. L., and Idol, W. K., *Chem. Eng. Commun.* **38**, 93 (1985).
7. Kraichnan, R. H., *Phys. Fluids* **13**, 22 (1970).
8. Gleeson, J. P., *Phys. Fluids* **12**, 1472 (2000).